FEBS Letters 350 (1994) 207–212

FEBS 14384

Substrate, substrate analogue, and inhibitor interactions with the ferrous active site of catechol 2,3-dioxygenase monitored through XAS studies

Ivano Bertini[a], Fabrizio Briganti[a], Stefano Mangani[b], Hans F. Nolting[c], Andrea Scozzafava[a,*]

[a]*Dipartimento di Chimica, Università di Firenze, Via Gino Capponi, 7, I-50121 Firenze, Italy*
[b]*Dipartimento di Chimica, Università di Siena, Pian dei Mantellini, 44, I-53100 Siena, Italy*
[c]*EMBL Outstation, DESY, Notkestraße, 85, W-2000 Hamburg 52, Germany*

Received 25 May 1994; revised version received 8 July 1994

Abstract

The interactions of catechol (substrate), 2-hydroxy-pyridine-*N*-oxide (substrate analogue), and 2-bromophenol (inhibitor) with the extradiol cleaving catechol-2,3-dioxygenase from *Pseudomonas putida* mt-2 have been monitored through X-ray absorption spectroscopy (XAS). The analysis of the data provides details about the mode of coordination of the substrate and of the inhibitors to the active site of the enzyme.

Key words: Catechol; Dioxygenase; EXAFS; Extradiol cleavage; *Pseudomonas putida*

1. Introduction

Catechol-2,3-dioxygenase (hereafter C2,3O) provides a critical step in the biodegradation pathways of a large share of environmental aromatic pollutants by catalyzing the extradiol opening of catechol rings and the insertion of molecular oxygen [1,2].

Such enzyme is encoded by the *xylE* gene of the TOL plasmid (pWW0) present in the bacterium Pseudomonas putida mt-2 [3,4]. Each of the four identical subunits (m.wt. 32,000) composing the enzyme contains one high spin iron(II) ion essential for activity.

Although this enzyme was isolated and crystallized for the first time in the early sixties [1,5–8], the structure of the active site is still unclear. No crystallographic data are available so far and Mössbauer spectroscopy has given very limited structural information, only suggesting that catechol binding does not alter the coordination environment of the high spin iron(II) ion [9].

Optical absorption, circular dichroism and magnetic circular dichroism techniques have also been applied proposing a five coordinate structure for iron(II) in the native enzyme and bidentate binding of catechol in the enzyme substrate adduct [8].

Further information has been obtained by studying through EPR, the inactive nitric oxide–enzyme complexes, which are characterized by a more easily EPR detectable S = 3/2 spin state. Hyperfine broadening of the EPR resonances of the nitrosyl complexes by ^{17}O-enriched H_2O showed that water is bound to iron and it is displaced by substrates [6].

In our laboratory we have approached the problem of the structural characterization of the active site of this enzyme through XAS and NMR spectroscopies.

^1H NMR data on the interaction of ortho-substituted phenols and aliphatic ketones were collected in order to obtain information on inhibitor–enzyme complexes. T_{iM}^{-1} (i = 1,2) paramagnetic enhancements to the relaxation rates are consistent with the direct binding of such compounds to the paramagnetic iron(II) center [10].

Previous XAS studies allowed us to reveal two histidines bound to the metal ion. Additional oxygen/nitrogen ligands complete the coordination sphere. The intensity of the pre-edge absorption has been suggested to be indicative of the coordination number. By comparison with the available data, the pre-edge absorption intensity is consistent with hexacoordination. Furthermore the metal geometry does not appear to be significantly affected by the binding of the inhibitor 2-chlorophenol [11]. EXAFS studies should not be considered to provide unequivocal structural data but as spectroscopic approach may be useful in providing structural patterns in a series of related systems.

In the present paper we extend the XAS studies on C2,3O to the characterization of the enzyme–substrate and enzyme–inhibitor adducts. For this reason we have collected XAS spectra of C2,3O in the presence of the substrate catechol, of the substrate analogue 2-hydroxy-pyridine-*N*-oxide, and of the inhibitor 2-bromophenol.

*Corresponding author. Fax: (39) (55) 2757555.

Abbreviations: C2,3O, Catechol-2,3-dioxygenase; EPR, electron paramagnetic resonance; EXAFS, extended X-ray absorption fine structure; NMR, nuclear magnetic resonance; XAS, X-ray absorption spectroscopy.

2. Materials and methods

The Pseudomonas putida bacterial strain mt-2 (ATCC 23973) was maintained on a minimal medium having meta-toluate as the exclusive

SSDI 0014-5793(94)00771-3

carbon source. Mass cultures and the enzyme purification were performed as previously described [3,6]. Catechol-2,3-dioxygenase activity and concentration were determined as previously reported [10]. The specific activity of the enzyme used in this study was greater than 300 units/mg.

X-ray absorption measurements were performed at the EMBL EXAFS beamline (c/o DESY, Hamburg), collected and analyzed as previously reported [11]. The data were collected at the iron edge (7,122.7 eV at the edge jump inflection point for all samples). The spectra were recorded from 6,912 to 7,812 eV with variable step widths. All the samples were run as frozen solutions at 20 K. EXAFS sample 1 was composed by a disaerated C2,3O 3.5 mM in Fe(II) solution to which was anaerobically added a catechol solution up to a final substrate concentration of 50 mM; sample 2 contained C2,3O 3.5 mM in Fe(II) additioned with 7 mM 2-hydroxy-pyridine-*N*-oxide; sample 3 contained C2,3O 3.5 mM in Fe(II) plus 35 mM 2-bromophenol. All the above reported samples were in 50 mM potassium phosphate buffer, pH 7.5, with 10% acetone. A series of 43, 49 and 34 spectra were collected for the catechol (sample 1), the 2-OH-pyridine-*N*-oxide (sample 2) and the 2-bromophenol (sample 3) complexes respectively. The data of sample 3 had to be cut at $k \cong 105$ nm^{-1} because of the presence of a discontinuity in the experimental spectrum. The other two data sets have been truncated at $k = 120$ nm^{-1}. The experimental spectra have been matched with the theoretical simulation by adjusting the parameter ΔE_0. The values determined were 14.10, 14.36 and 12.15 eV for samples 1, 2 and 3 respectively. This resulted in putting the experimental absorption edge at $k \approx 0.18$ nm^{-1}. The above values were kept fixed during all subsequent simulations. The energy independent amplitude reduction factors were determined and kept fixed at 0.71, 0.82, 0.73 for samples 1, 2 and 3 respectively. The Fourier transforms were calculated over the k range 25–120 (105 for sample 3) nm^{-1}. Gaussian windows were used for Fourier backtransforms. The distance ranges used in the backtransforms are listed in the figures and table captions.

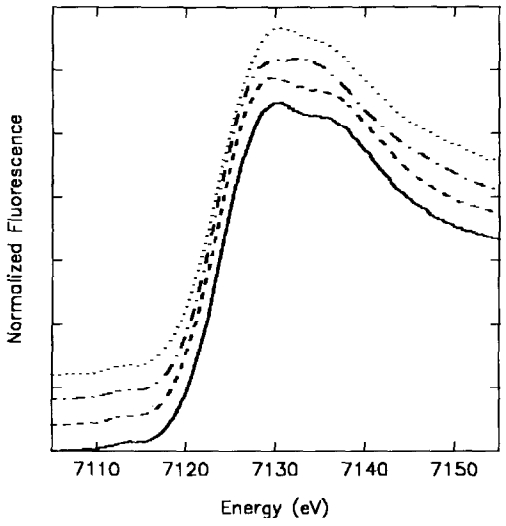

Fig. 1. Edge spectra of C2,3O samples: Catechol–C2,3O enzyme complex (· · · · · · ·), 2-hydroxy-pyridine-*N*-oxide–C2,3O enzyme complex (-·-·-·-), 2-bromophenol–C2,3O enzyme complex (- - - - - -) and (taken from [11]) native C2,3O (————————).

3. Results

3.1. Edge data

The edge position remains constant at 7,122.7 eV for all of the three samples. The comparison with the native enzyme shows that the iron oxidation state has not changed upon ligand binding and that is +2 in every case (Fig. 1). A characteristic pre-edge peak appears in the iron K-edge spectra at about −10 eV from the edge. This peak is due to a transition to bound states (1s–3d) which is forbidden by the spectral selection rules. Its presence can be interpreted in terms of quadrupole and symmetry breaking effects [12,13]. The intensity of this transition is correlated to the iron coordination geometry [14,15] and increases with the deviation from centrosymmetry of the complex. The values obtained for the substrate, substrate-analogue and inhibitor complexes of C2,3O are 0.043, 0.049 and 0.048 eV respectively. The intensities of the 1s–3d transition obtained from octahedral ferrous model complexes range typically from 0.03 to 0.07 eV [11] whereas the pre-edge peak areas of five coordinate Fe(II) models have been found between 0.089 and 0.107 eV [15]. Since the intensity for the native enzyme is 0.058 the present results indicate that the overall symmetry is unchanged upon substrate and inhibitor binding and that the iron (II) site remains octahedral.

3.2. EXAFS data

The filtered k^3 weighted experimental EXAFS spectra of the three samples are reported for comparison in Fig. 2. The interaction with the different ligands deeply perturbs the EXAFS spectrum (see [11] for comparison with the native enzyme). This evidence taken together with the changes occurring in the XANES region is consistent

Table 1
One and two distance fits of the first Fe(II) iron coordination shell of native C2,3O and the catechol, 2OH-pyridine-*N*-oxide, and 2Br-phenol complexes with C2,3O[1]

Native C2,3O[2]					C2,3O-Catechol complex					C2,3O-2OH-Pyridine-N-oxide complex					C2,3O-Bromophenol complex				
Shell 1	Shell 2	R (nm)	$2\sigma^2\times10^4$ (nm^2)	F1	Shell 1	Shell 2	R (nm)	$2\sigma^2\times10^4$ (nm^2)	F1	Shell 1	Shell 2	R (nm)	$2\sigma^2\times10^4$ (nm^2)	F1	Shell 1	Shell 2	R (nm)	$2\sigma^2\times10^4$ (nm^2)	F1
6 O/N		0.205	2.2	0.1	6O/N		0.200	1.8	0.16	6O/N		0.201	2.0	0.15	6O/N		0.204	1.8	0.46
4O		0.202	1.4	0.05	4O		0.197	1.1	0.13	4O		0.198	1.2	0.08	4O		0.202	1.5	0.42
	2N	0.217	1.5			2N	0.211	0.7			2N	0.213	0.6			2N	0.214	0.7	
3O		0.201	0.7	0.09	3O		0.196	0.6	0.30	3O		0.197	0.6	0.30	3O		0.201	0.7	0.49
	2N	0.217	0.4			2N	0.211	0.1			2N	0.213	0.1			2N	0.215	0.2	

[1] e.s.d. on distances = ± 0.002 nm. [2]Data taken from reference 11.

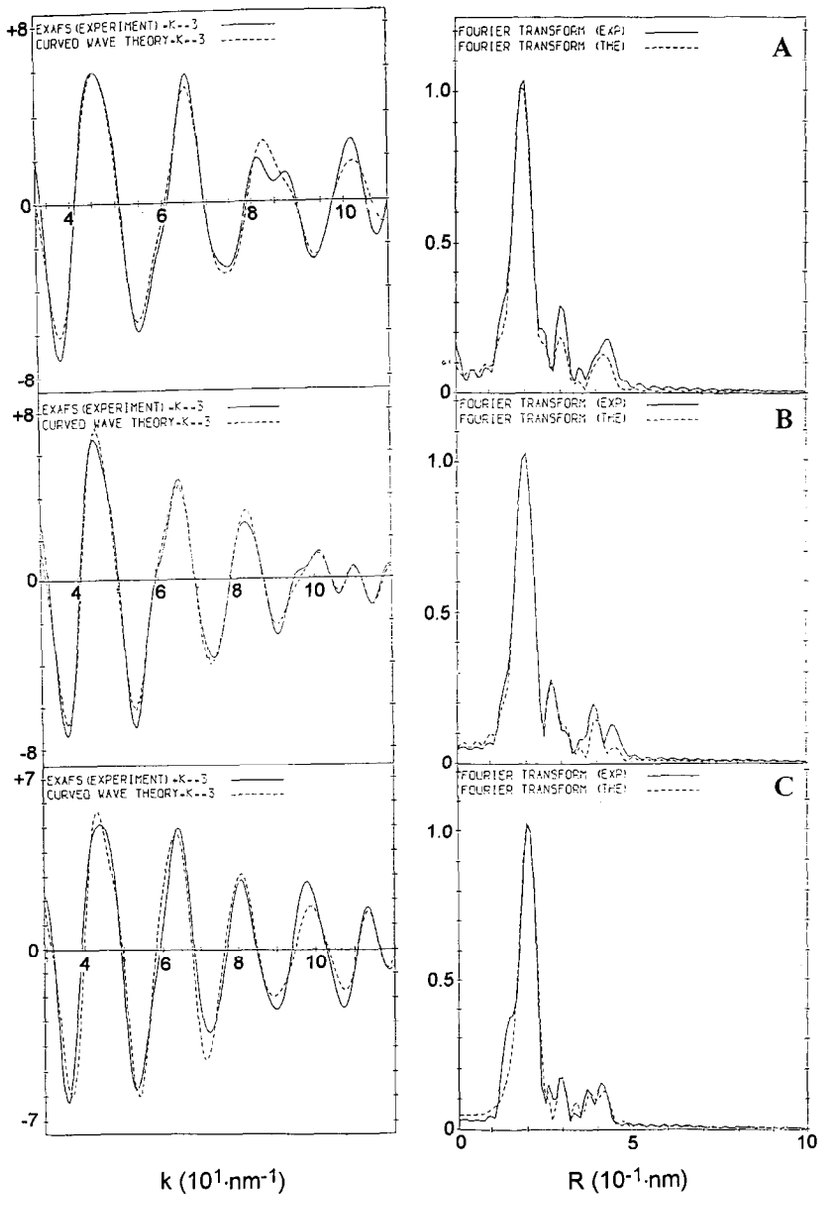

Fig. 2. k^3 weighted filtered (between 0.10 and 0.41 nm) (————) and calculated (- - -) EXAFS spectra with the respective Fourier transforms for the (a) Catechol–C2,3O enzyme complex, (b) 2-hydroxy-pyridine-*N*-oxide–C2,3O enzyme complex, and (c) 2-bromophenol–C2,3O enzyme complex.

with the direct binding of the ligands to the iron center. The changes mainly affect the iron outer shells atomic distribution as shown by the different disposition of the outer peaks in the spectra Fourier transforms (FT) (Fig. 2).

The features appearing in the EXAFS between 40 and 65 nm^{-1} are characteristic of imidazole backscattering. The presence of such type of ligands is also revealed in the spectra Fourier transforms by the peaks present at about 0.28–0.30 and 0.40–0.43 nm. However the different complex peak patterns in the three samples suggest that the Fe(II) ligands have different spatial arrangements.

3.3. *First shell analysis*

The iron first coordination shell has been analyzed by Fourier filtering the nearest neighbours contribution and by backtransforming it to k space. The results are reported in Table 1. Attempts to simulate the first shell with a single metal-to-ligand distance have been made using five or six O/N atoms. The large values obtained for the Debye-Waller factors in every case suggest that a large spread of distances is present in the iron(II) first coordination shell; hence two distance fits were performed. All the possible combinations of oxygen and nitrogen atoms summing up to five and six were used. The best results are reported in Table 1. The splitting of

the Fe-ligand distances in two ranges improves significantly the quality of the fit for the catechol and the 2OH-pyridine-*N*-oxide complexes. From Table 1 it can be seen that the quality of both one- and two-distance fits of the 2-bromophenol inhibitor spectrum is not as high as that of the other complexes. This is due to the lower counting statistics of the sample 3 data and to the shorter data range usable. In any case the best results were obtained with the higher coordination number.

3.4. Outer shell analysis

The substrate and inhibitor–enzyme complex formation causes remarkable changes in the spectra FT's outer shells peaks distribution with respect to the native enzyme. Variation in the XANES peaks is also observed (Fig. 1).

The peaks in the 0.28–0.43 nm range in the FT of the three samples can be due to the presence of histidine residues, of the aromatic rings of the substrate/inhibitor and to the carbon atoms of the side chains of the other iron ligands. In order to estimate the number of histidine groups and to monitor the mode of binding of the different exogenous ligands we have performed a multiple scattering analysis coupled to constrained refinement on spectra Fourier filtered between 0.1 and 0.44 nm. Such approach has been proven to be able to account for these features both for protein and model compounds data [16–19]. Fig. 2 shows that the main features of the spectra and of the Fourier transforms of the various substrate/inhibitor–C2,3O complexes could be quite accurately reproduced by introducing in the simulation all the atoms of two imidazole rings and those of the exogenous ligand in addition to the other first shell atoms.

The complex with the substrate catechol (sample 1) was modelled as an iron(II) bound to two histidine imidazole nitrogens and four oxygen atoms, two of them belonging to the bidentate catechol molecule (see Fig. 3A). In addition to all the atoms of the two imidazole rings two additional shells, corresponding to the two

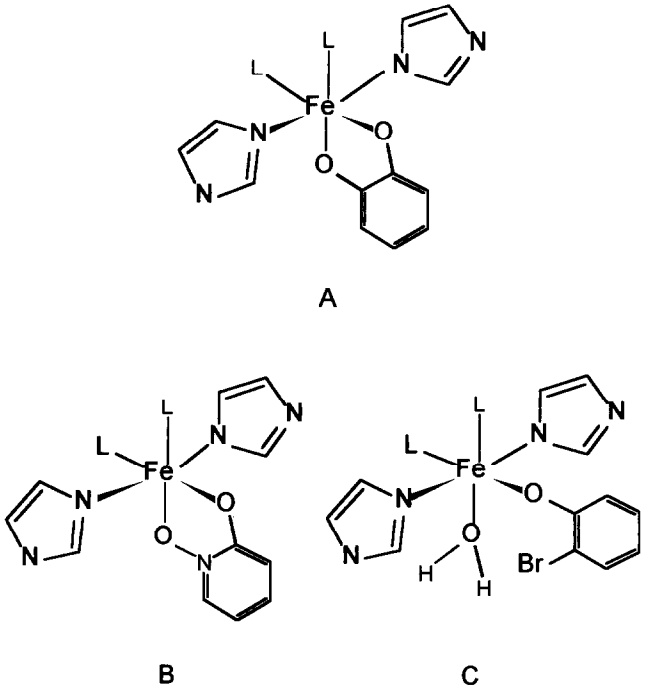

Fig. 3. Schemes of the active Iron(II) coordination sites in: (a) Catechol–C2,3O enzyme complex, (b) 2-hydroxy-pyridine-*N*-oxide–C2,3O enzyme complex, and (c) 2-bromophenol–C2,3O enzyme complex. L represents N/O donors. The *trans*- arrangement of the histidine ligands is just a pictorial representation. The water molecule in (c) derives from [5].

C1,C2 and C3, C4 carbon shells of catechol, were added to simulate the peaks present in the FT at 0.280 and at 0.408 nm respectively (see Table 2). The complex with the substrate analogue 2OH-pyridine-*N*-oxide (sample 2) was designed in a similar way with the analogue molecule substituting the catechol as a slightly asymmetric ligand (see Fig. 3B). The spectrum was simulated introducing the N1 and C1 atoms of the 2-OH-pyridine-*N*-oxide ring at 0.280 and 0.283 nm, respectively, and a further shell

Table 2
Parameters used to simulate the Fourier filtered (0.10–0.41 nm) data of catechol, 2OH-pyridine-*N*-oxide, and 2-bromophenol complexes with C2,3O as reported in the figures[1]

C2,3O-Catechol complex FI = 0.80			C2,3O-2OH-Pyridine-N-oxide complex FI = 0.42			C2,3O-Bromophenol complex FI = 1.32		
Shell	R (nm)	$2\sigma^2 \times 10^4$ (nm^2)	Shell	R (nm)	$2\sigma^2 \times 10^4$ (nm^2)	Shell	R (nm)	$2\sigma^2 \times 10^4$ (nm^2)
4O	0.197	1.1	4O	0.198	1.3	4O	0.202	1.3
*2N	0.211	1.0	*2N	0.213	0.8	*2N	0.214	0.7
2C	0.280	1.8	1N	0.280	0.4	1C	0.302	1.3
*2C	0.299	0.2	1C	0.283	0.2	*2C	0.305	1.4
*2C	0.324	1.2	*2C	0.302	0.2	*2C	0.327	0.2
2C	0.408	1.2	*2C	0.325	0.6	2C	0.380	0.7
*2C	0.420	0.2	2C	0.419	0.8	1Br	0.420	1.6
*2N	0.429	1.6	*2C	0.422	0.1	*2C	0.425	1.5
			*2N	0.430	1.8	*2N	0.433	1.2

[1] e.s.d. on distances = ± 0.002 nm. The asterisk refers to the atomic shells describing the imidazole groups.

composed by the C2 and C3 atoms of the same molecule ring at 0.419 nm (see Table 2). The multiple scattering contributions of the catechol and of the 2OH-pyridine-*N*-oxide bound bidentate to the iron ion have been calculated and found scarcely influencing the spectra simulations. In the case of the 2-bromophenol–enzyme complex (sample 3) the monodentate binding of the inhibitor through the phenolate oxygen was assumed (see Fig. 3C). In this case the phenol ring should not contribute to multiple scattering effects being tilted of about 110–120° with respect to the Fe–O bond and the torsion angle Fe-*O*-C1(phenol)-C2(phenol) being somewhere between 100° and 120° (i.e. Fe, O, C1, C2 not in the same plane). These values are observed in the crystal structures of Fe(III)-phenolate complexes [20] and of the protein lactoferrin [21]. Indeed such a model, added to the multiple scattering contributions from two imidazole rings, is able to reproduce all the features of the EXAFS spectrum and of its FT. This model also includes one bromine atom at 0.420 nm, one carbon atom at 0.302 nm accounting for the C1 phenolate carbon (superimposed with the imidazole C2–C5 shells) and a further shell of two carbon atoms at 0.380 nm which may account for the phenolate C2 and C6 carbons. The peak at 0.42 nm bears contributions from the outer imidazole shells and the putative bromine atom meaning that our model of monodentate binding of the inhibitor is consistent with the experimental data. Attempts to simulate the data from samples 1 and 2 with a monodentate catechol and 2-OH-pyridine *N*-oxide ligands resulted in significantly worse fits and were not able to reproduce all the EXAFS features.

4. Discussion

The pre-edge peak intensities as well as the EXAFS data strongly indicate that the coordination number (six) and the geometry remain essentially unchanged in all the studied complexes with respect to the native enzyme. As the spectral analysis in every case reveals evidences of two histidines coordinated to the metal ion, it seems that water molecules or other proteic ligands are displaced by the substrate/substrate-analogues molecules. Any attempt to fit the spectra with less than six ligands resulted in significantly higher fit indexes and worse visual matches.

A systematic increase in the average first shell distance going from the catechol to the 2-hydroxy-pyridine-*N*-oxide and the 2-bromophenol complexes is observed. As shown in Table 1, the first shell average distances are always shorter than the distances found in the native enzyme (reported in Table 1 for comparison), the catechol complex exhibiting the shortest. All the observed distances are in the lower limit of the Fe-O and Fe-N(His) distances; the same has been observed also in the case of the native lipoxygenase [22,23] and isopenicillin-*N*-synthase [15,24]; similar distances have also been found in several Fe(II) model compounds [25–30].

It must be kept in mind that it is unsafe to draw firm conclusions about the configuration of the Fe(II) ligands based solely on the results of the above fitting analysis. However it is possible to state that a model containing bidentate complexes of the catechol and 2-hydroxy-pyridine-*N*-oxide adducts to the active site iron ion is consistent with the experimental data whereas a monodentate model was unable to give satisfactory results. As a matter of fact the relative height of the second shell peak centered at about 0.3 nm is decreasing from the catechol to the 2-hydroxy-pyridine-*N*-oxide and the 2-bromophenol adduct in agreement with the presence of a symmetric bidentate catechol ligand, an asymmetric bidentate ligand, and a monodentate ligand, respectively. In fact a bidentate catechol will contribute to the EXAFS signals with two aromatic carbon atoms at about 0.28 nm whereas in the asymmetric 2-hydroxy-pyridine-*N*-oxide ligand this shell will be split into two slightly different distances with consequent partially destructive interference and finally in the monodentate binding case we expect the contribution of only one carbon at 0.30 nm.

In Fig. 3 the schemes representing the active site metal ion of C2,3O in the presence of substrate or inhibitors as appear from the analysis of the XAS data are reported. Our data appear to be in agreement with the Mössbauer data indicating a substitutional variability at the metal center without affecting the coordination number [9]. Furthermore the present data on the substrate and the substrate analogue–C2,3O complexes should be relevant for the elucidation of the catalytic mechanism since they point out that the bidentate binding of such molecules to the active site iron ion could be an essential feature for a productive enzyme–substrate complex formation in the extradiol cleaving catalytic process.

Acknowledgements: The authors would like to acknowledge the use of technical facilities within the laboratories of the MASIMO network and the European Union Human Capital and Mobility Grant ERBCHRXCT920072.

References

[1] Lipscomb, J.D. and Orville, A.M. (1992) in: Metal Ions in Biological Systems, Vol. 28 (Sigel, H. and Sigel A. eds.) Ch. 8, pp. 243–298, Marcel Dekker Inc., New York.
[2] Que Jr., L. (1989) in: Iron Carriers and Iron Proteins (T. Loehr, Ed.) pp. 467–524, VCH, New York.
[3] Nakai, C., Hori, K., Kagamiyama, H., Nakazawa, T. and Nozaki, M. (1983) J. Biol. Chem. 258, 2916–2922.
[4] Assinder, S.J. and Williams, P.A. (1990) Adv. Microb. Phys. 31, 1–69.
[5] Arciero, D.M., Lipscomb, J.D., Huynh, B.H., Kent, T.A. and Münck, E. (1983) J. Biol. Chem. 258, 14981–14991.
[6] Arciero, D.M., Orville, A.M. and Lipscomb, J.D. (1985) J. Biol. Chem. 260, 14035–14044.

[7] Arciero, D.M. and Lipscomb, J.D. (1986) J. Biol. Chem. 261, 2170–2178.
[8] Mabrouk, P.A., Orville, A.M., Lipscomb, J.D. and Solomon, E.I. (1991) J. Am. Chem. Soc. 113, 4053–4061.
[9] Tatsuno, Y., Saeki, Y., Nozaki, M., Otsuka, S. and Maeda, Y. (1983) FEBS Lett. 112, 83–85.
[10] Bertini, I., Briganti, F. and Scozzafava, A. (1994) FEBS Lett. 343, 56–60.
[11] Bertini, I., Briganti, F., Mangani, S., Nolting, H.-F. and Scozzafava, A. (1994) Biochemistry, in press.
[12] Shulman, R.G., Yafet, Y., Eisenberger, P. and Blumberg, W.E. (1976) Proc. Natl. Acad. Sci. USA 73, 1384–1388.
[13] Roe, A.L., Schneider, D.J., Mayer, R.J., Pyrz, J.W., Widom, J. and Que Jr., L. (1984) J. Am. Chem. Soc. 106, 1676–1681.
[14] Priggemeyer, S. (1991) PhD dissertation thesis, Westfälischen Wilhelms-Universität zu Müster, Germany.
[15] Randall, C.R., Zang, Y., True, A.E., Que Jr., L., Charnock, J.M., Garner, C.D., Fujishima, Y., Schofield, C.J. and Baldwin, J.E. (1993) Biochemistry 32, 6664–6673.
[16] Binsted, N., Stranger, R.W. and Hasnain, S.S. (1992) Biochemistry 31, 12117–12125.
[17] Bunker, G., Stern, E.A., Blakenship, R.E. and Parson, W.W. (1982) Biophys. J. 37, 539–551.
[18] Pettifer, R.F., Foulis, D.L. and Hermes, C. (1986) J. Phys. C8, 545–550.
[19] Hasnain, S.S. and Strange, R.W. (1990) in Biophysics and Synchrotron Radiation (Hasnain S.S. Ed.) p. 104 Ellis Horwood Ltd., Chichester, UK.
[20] Koch, S.A. and Millar, M. (1982) J. Am. Chem. Soc. 104, 5255–5257.
[21] Anderson, B.F., Baker, H.M., Norris, G.E., Rice, D.W. and Baker, E.N. (1989) J. Mol. Biol. 209, 711–734.
[22] Navaratnam, S., Feiters, M.C., Al-Hakim, M., Allen, J.C., Veldink, G. and Vliegenthart, F.G. (1988) Biochim. Biophys. Acta 956, 70–76.
[23] Van der Heijdt, L.M., Feiters, M.C., Navaratnam, S., Nolting, H.F., Hermes, C., Veldink, G. and Vliegenthart, F.G. (1992) Eur. J. Biochem. 207, 793–802.
[24] Scott, R.A., Wang, S., Eidsness, M.K., Kriauciunas, A., Frolik, C.A. and Chen, W.J. (1992) Biochemistry 31, 4596–4601.
[25] Borovik, A.S., Hendrich, M.P., Holman, T.R., Münk, E., Papaefthymiou, V. and Que Jr., L. (1990) J. Am. Chem. Soc. 112, 6031–6038.
[26] Rakotonandrasana, A., Boinnard, D., Savariault, J.-M., Tuchagues, J.-P., Petrouleas, V., Cartier, C. and Verdaguer, M. (1991) Inorg. Chim. Acta 180, 19–31.
[27] Martinez-Lorente, M.A., Tuchagues, J.P., Petruleas, V., Savariault, J.M., Poinsot, R. and Drillon, M. (1991) Inorg. Chem. 30, 3587–3589.
[28] Ménage, S., Zang, Y., Hendrich, M.P. and Que Jr., L. (1992) J. Am. Chem. Soc. 114, 7786–7792.
[29] Chiou, Y. and Que Jr., L. (1992) J. Am. Chem. Soc. 114, 7567–7568.
[30] Zang, Y., Elgren, T.E., Dong, Y. and Que Jr., L. (1993) J. Am. Chem. Soc. 115, 811–813.